A NEW PERSPECTIVE ON WALL-MODELLED LARGE-EDDY SIMULATIONS

Stefan Wallin
Division of Fluid Mechanics & FLOW
KTH
SE-100 44 Stockholm, Sweden
stefanw@mech.kth.se

ABSTRACT

A new wall boundary condition for wall-modelled LES is proposed, formulated as a Robin condition derived from a Reynolds-number scaling based on a computational viscosity (molecular + SGS). The approach interprets LES as a surrogate low-Re flow and enforces outer-layer similarity. The model is validated using RANS and LES of high-Re channel flow across a wide range of resolutions and friction Reynolds numbers between 250 and 20 000. The method generates resolved near-wall turbulence mitigating numerical transition and reduces log-layer mismatch. It remains robust down to extremely coarse grids (less than 20 000 cells).

INTRODUCTION

Large-eddy simulation of high-Reynolds number wall bounded flows requires special near-wall treatment to be of practical interest. Wall modelling in terms of log-law related wall functions or two-layer approaches, e.g. hybrid RANS/LES, is an active research field. Some of the basic problems related to these approaches are log-layer mismatch, artificial buffer layer, and unphysical near-wall turbulence.

Most solutions presented so far to deal with these problems are attacking the consequences of the poor near-wall resolution by bridging ideas or by ad-hoc forcing the flow to adhere to the expected high-Re results. For example, wall functions for LES are usually monitoring the velocity at some distance from the wall, where the turbulent flow is assumed to be fully developed, for estimating the wall shear stress to be used for the log-law boundary condition. Hence, the near wall LES solution will be biased toward the imposed log law. Moreover, the relatively large distance to the monitoring position requires elaborated higher order or non-trivial differential log laws.

The resolved flow associated with wall-modelled LES of high-Re flows has similarities with low-Re turbulent flows. In fact, an LES can be considered as a DNS of a particular non-Newtonian fluid, an “LES fluid”, as stated by Muschinski (1996). Reyes, Cooper & Girimaji (2014) found that the scale-resolved turbulence scales with the computational viscosity (e.g. $\nu^* = \nu + \nu_{SGS}$) consistent with $Re_c = UL/\nu^*$. For example, the spanwise spacing of the artificial streaks is typical around $100l^*$ and the position of the buffer layer around $20l^*$ where $l^* = \nu^*/u_\tau$ is the computational viscous wall unit, which can be verified from numerous LES.

In this work, LES is interpreted as a DNS of a surrogate fluid with viscosity $\nu^* = \nu + \nu_{SGS}$. Based on this interpretation, we derive a wall boundary condition from Reynolds-number similarity rather than imposing a log-law constraint.

THE SURROGATE SETUP

Let us embrace the consequences of that we are in fact simulating low-Re flows. Let us also think about the “LES fluid” as a real, but artificial, surrogate fluid. Hence, the problem of wall-modelled LES of a high-Re flow is then replaced by the problem of finding a fluid and setup that best represents the original high-Re flow. The numerical solution then becomes unproblematic. The entangling of numerics and physical modelling in LES will then be decomposed and separated.

Let us study the log layer of a typical high-Re boundary layer of our interest and the surrogate flow, denoted by U and V respectively. We impose the requirement that they will be similar in outer scaling having the same skin friction (or u_τ). $U^+(y^+)$ and $V^*(y^*)$ represent inner scaling by ν and ν^* respectively. For the high-Re flow we have

$$U^+ = \frac{1}{\kappa}\ln(y^+) + C, \tag{1}$$

where κ is the von Karman constant around 0.4 and using the wall scaling

$$U^+ = \frac{U}{u_\tau}, \qquad y^+ = \frac{u_\tau y}{\nu}. \tag{2}$$

Now, we can define the log layer for the surrogate flow. For reasons that will be clear further down, we will for the surrogate setup introduce an arbitrary wall slip V_s^* and an arbitrary wall roughness denoted by a log shift D^* as well. Hence,

$$V^* - V_s^* = \frac{1}{\kappa}\ln(y^*) + C - D^*, \tag{3}$$

with the surrogate wall scaling based on the LES computational viscosity ν^*.The first requirement on the surrogate setup is that the skin friction is the same as for the real high-Re case, or $v_\tau = u_\tau$. Hence $V^* = V^+$. Eqs. (1) and (3) in outer scaling then become

$$U^+ = \frac{1}{\kappa}\ln\left(\frac{y}{\delta}\right) + C', \qquad C' = \frac{1}{\kappa}\ln(\delta^+) + C \tag{4}$$

and

$$V^+ - V_s^+ = \frac{1}{\kappa}\ln\left(\frac{y}{\delta}\right) - \frac{1}{\kappa}\ln\left(\frac{\nu^*}{\nu}\right) + C' - D^+. \tag{5}$$

Finally, outer-layer similarity $U^+(y/\delta) = V^+(y/\delta)$ will result in

$$V_s^+ = \frac{1}{\kappa}\ln\left(\frac{\nu + \nu_{SGS}}{\nu}\right) + D^+. \tag{6}$$

This relation defines the wall slip velocity solely from local quantities through the ratio ν^*/ν, making the boundary condition independent of outer flow variables.

We can here note that we have made no assumptions concerning the wake – only that the inner layer of the flow will approach a log layer. Hence, the scaling should be reasonable in different flows with different pressure gradients and Reynolds numbers.

The surrogate setup is now defined as a wall slip velocity V_s^+ defined from a simple Reynolds number scaling in terms of the LES computational viscosity ν^* at the wall. Interesting to note is that the wall slip is derived from similarity in outer scaling.

Moreover, V_s^+ is represented by known quantities independent of the outer flow, but resolution and Re dependent through ν^*/ν.

Moreover, an arbitrary roughness parameter D^+ may be introduced for the surrogate setup. We should make clear that the high-Re flow of interest is assumed to have no wall roughness.

THE SURROGATE RANS SOLUTION

The concept of the surrogate flow can be tested by RANS by solving for the low-Re surrogate mean flow with variable viscosity, ν^*. Here, we define the viscosity ν^* as

$$\nu^* = \nu + \nu_{SGS} \text{ where } \nu_{SGS} = (C_S\Delta)^2|S| \qquad (7)$$

where S is approximated by $\partial V/\partial y$ from the solution. The RANS solution is well resolved and the filter size Δ is just imposed as a parameter. A slip wall boundary condition is introduced with the slip velocity according to (6).

The RANS solutions of fully developed channel flow at Re_τ=10.000 using SST k-ω for the surrogate setup is shown in Figure 1 with three different Δ corresponding to 10, 20 and 50 cells through the half channel. Wall roughness $D^+ = 5.3$ is introduced for the surrogate setup, which corresponds to a roughness height of a fraction of the grid resolution $k_s \approx 0.4\Delta$. Comparison without wall roughness is made as well.

All surrogate solutions fit well to the high-Re outer solution and similarity is remarkably improved by wall roughness. Noticeable is that all RANS results show almost identical centre-line velocities in plus units, which means that the skin-friction coefficient is matched. This demonstrate that the wall slip relation for V_s^+ is valid.

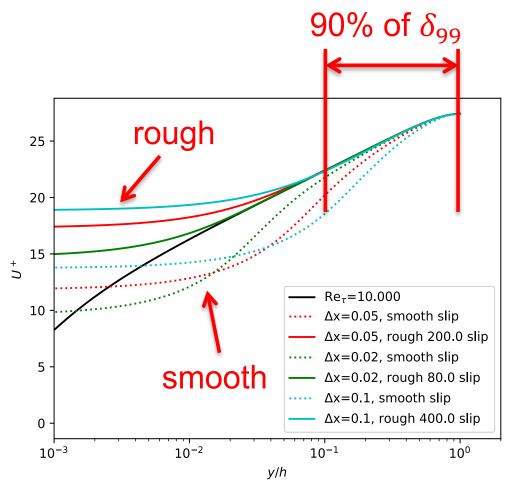

Figure 1. RANS solutions of surrogate "LES fluid" for fully developed channel flow at Re_τ=10 000.

These results confirm the classical Townsend similarity hypothesis (1977) stating: "Outside the roughness (or viscous) sublayer, turbulence (and its action) is independent of viscosity and wall roughness in outer scaling. If Re is sufficiently high." This can be interpreted as the reason for that LES is working. That LES, which is in fact a low-Re DNS, can accurately represent the high-Re flow in outer scaling. And, also, the reason for that the near-wall region cannot be well represented by LES. Hence, for each high-Re flow there exists a surrogate setup with similar mean flow and turbulence in most of the boundary layer except for the very near-wall region.

Surrogate wall roughness will enhance the low-Re turbulence and increase the effective Re_c but must be compensated by increased slip V_s. Moreover, "sufficiently" high Re_c can be directly translated to the resolution Δ replacing empirical statements like "at least 80% of the TKE must be resolved". Sufficiently high $Re_{\tau,c}$ is in the order of 100 which directly is translated into a resolution requirement through the ν^* definition.

THE SURROGATE DNS (WALL-MODELLED LES)

The DNS of the surrogate setup will in practice be an LES with a particular slip-wall boundary condition. So far, the analysis is independent on the choice of SGS model, only ν_{SGS} is needed. Firstly, the slip BC need to be elaborated. V_s^+ is known from (6) but the friction velocity, u_τ, is needed for the dimensional slip velocity, V_s.

To apply the slip condition in LES, we eliminate u_τ using the SGS viscosity model, resulting in a local relation between velocity and its wall-normal gradient.

First, we expand $u_\tau^2 = \nu^* S_w = (C_S\Delta)^2 S_w^2$ using e.g. Smagorinsky, where $S_w = \partial V/\partial y$. This will result in $V_s = C_S\Delta S_w V_s^+$, which, in fact, is a relation between the slip velocity and its gradient at the wall – a Robin BC. Moreover, the relation will be written in terms of the instantaneous resolved tangential velocity, $v_{t,i}$

$$v_{t,i} = L_s \frac{\partial v_{t,i}}{\partial n}, \qquad L_s = C_S\Delta \mathrm{V}_s^+ \qquad (8)$$

where the slip length L_s is formulated in terms of V_s^+ according to (6) and C_S and Δ are the Smagorinsky coefficient and filter size respectively. For the smooth surrogate solution, the wall-normal component will be zero and the slip length L_s is applied only for the tangential component of the wall velocity with $L_s = C_S\Delta \mathrm{V}_{s0}^+$, where $\mathrm{V}_{s0}^+ = \mathrm{V}_s^+(D^+ = 0)$.

Introducing wall roughness

The RANS study shows, consistent with Townsend similarity hypothesis, that introducing wall roughness for the surrogate setup will improve the similarity in outer scaling. Alternatively, relaxing the resolution requirement for similar results. So, how can we introduce wall roughness in the LES of the surrogate setup? Statistically, wall roughness is consistent with wall-normal velocity fluctuations. The transpiration-resistance model (TRM) was proposed by Lācis et al (2020), see also Habibi Khorasani et al (2022), where they show that the introduction of a Robin BC with both tangential and wall-normal slip length can be used for simulating wall micro-structures in DNS. Moreover, Lozano-Durán & Bae (2019) confirmed that the Townsend similarity hypothesis for the outer scaling indeed is fulfilled also with such a penetration boundary condition.

Hence, we will adopt such Robin BC also for the wall-normal velocity component. The proposed formulation has the following form

$$v_{t,i} = L_s \frac{\partial v_{t,i}}{\partial n}, \qquad v_{n,i} = L_n \frac{\partial v_{n,i}}{\partial n} \qquad (9)$$

where $v_{t,i}$ and v are the tangential and wall-normal resolved velocity components. The length scales have the following form

$$L_s = C_S\Delta \mathrm{V}_s^+, \qquad L_n = C_S\Delta \mathrm{V}_n^+, \qquad (10)$$

where

$$\mathrm{V}_s^+ = \mathrm{V}_{s0}^+ + D_t^+ f_d, \qquad \mathrm{V}_n^+ = D_n^+ f_d,$$
$$\mathrm{V}_{s0}^+ = \frac{1}{\kappa}\ln\left(\frac{\nu + \nu_{SGS}}{\nu}\right). \qquad (11)$$

The length scales now have two different purposes: i) to introduce the Reynolds number scaling between the real flow and surrogate setup through V_{s0}^+ and ii) to model the surrogate wall roughness through the D_t^+ and D_n^+ parameters. Moreover, the amount of wall roughness in the surrogate setup should vanish when the resolution is approaching DNS of the real case. In the DNS limit, $\nu^* \rightarrow \nu$ and $V_{s0}^+ \rightarrow 0$ and the function f_d should approach zero. Our first attempt is

$$f_d = \min\left(1, \frac{V_{s0}^+}{C_{s0}^+}\right) \tag{12}$$

where C_{s0} is a parameter.

SOME RESULTS FOR CHANNEL FLOW

First calibrations are made by simulating fully developed high-Re channel flow as a DNS of a surrogate LES fluid at a much lower Reynolds number given by Re_c together with the Robin BC. Or, in other words, an LES with the new wall BC. The domain size is $2\pi h \times 2h \times \pi h$ and is driven by a constant bulk velocity. Smagorinsky SGS model is used with C_S=0.2. The convective CFL number $CFL_c = \Delta t U_b/\Delta x$=0.2. Results using the present Slip BC is compared with standard equilibrium WF where the wall skin friction is derived from the instantaneous velocity at the first inner node.

Different Re_τ ranging from 250 to 20 000 are computed for different quite coarse resolutions given in Table 1. The coarsest grid is included for exploring the limits and consists of about 2 000 cells in total. Which is ridiculously coarse considering that a standard generic 2nd order accurate CFD solver is used.

Table 1. Channel grid resolution.

name	$n_x \times n_y \times n_z$	$\Delta_x^+ \times \Delta_y^+ \times \Delta_z^+$
f	120×80×120	270×100×135
m	60×40×60	540×220×270
c	30×20×30	1100×500×550
xc–	15 × 10× 15	2200 × 1000 × 1100

The preliminary calibration gives the following set of parameters; $D_t^+ = 8.3$, $D_n^+ = 7.0$ and $C_{s0}^+ = 6.0$. Moreover, $\kappa = 0.41$ was used.

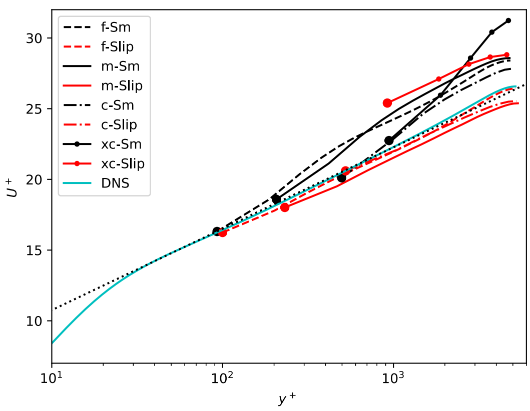

Figure 2. Mean velocity by the new Slip BC (red) compared with standard WF (black) and DNS for different resolutions at Re_τ=5 200. The large dots represent the solutions in the first inner point.

Influence of resolution

First, we will show the influence of the resolution for $Re_\tau = 5\,200$. The mean velocity is shown in Figure 2. The standard LES shows the typical log-layer mismatch, but the new BC shows a different behaviour with a much better match with the log layer. Moreover, the different resolutions collapse across resolutions, indicating weak sensitivity to resolution in outer scaling. Even the coarse c with only 18.000 cells. In fact, the extra coarse xc with 2.000 cells shows a fair amount of resolved turbulence while the WF BC is almost steady.

The resolved Reynolds shear stress $\overline{u'v'}$ in Figure 3 shows that there is a turbulent momentum flux present already at the boundary implying that there is production of resolved turbulence there. This means that there are wall-normal fluctuations present that are correctly correlated with the wall-tangential fluctuations. The spanwise fluctuations $\overline{w'w'}$ are shown in the same figure, which are related to 3D well developed turbulence. More developed near-wall turbulence is present with the new Slip BC, in particular for the coarser resolutions.

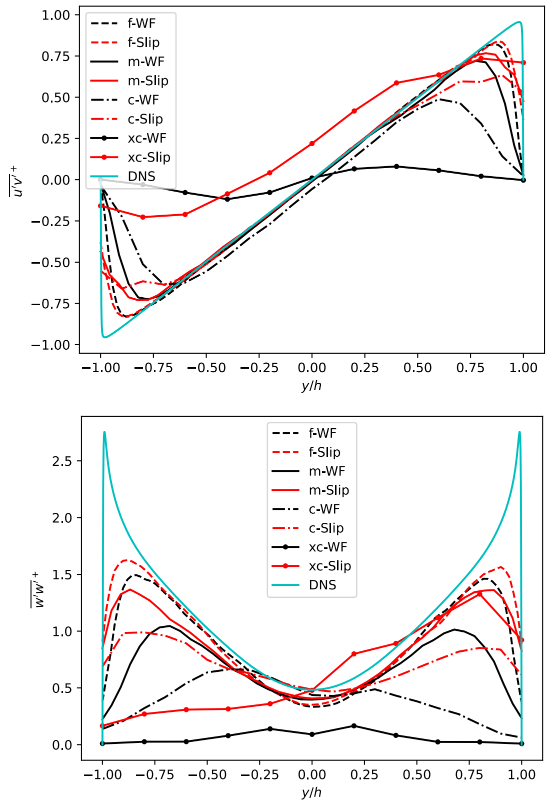

Figure 3. The resolved shear stress $\overline{u'v'}$ (top) and spanwise fluctuations $\overline{w'w'}$ (bottom) (as Figure 2).

The same conclusion can be drawn from Figure 4 where all parts of the shear stress are shown; resolved ($\overline{u'v'}$), SGS ($\nu_{SGS}\partial u/\partial y$) and viscous ($\nu\partial U/\partial y$). The new Slip BC introduces resolved wall shear stress, which is balanced by reduced SGS stress, which are almost equal at the wall. The wall SGS and resolved stresses are similar for all different resolutions.

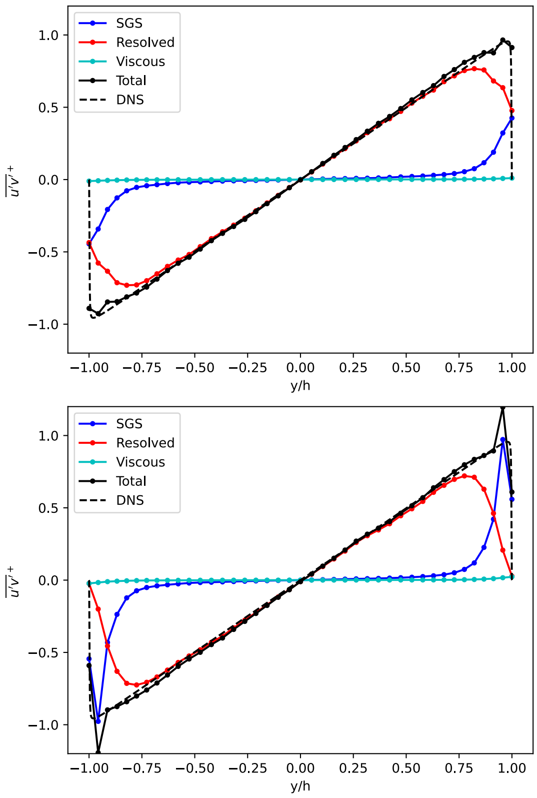

Figure 4. The different shear-stress components for the new Slip BC (top) and standard WF (bottom) for the medium m mesh. The same settings as in Figure 2.

Reynolds-number influence

The next study is to vary the Reynolds number for a constant medium m resolution. The range of Re_τ is quite large from 250 to 20 000. The mean velocity is shown in Figure 5 where, also here, we see the typical log-layer mismatch for the standard WF results and a much better match with the log layer for the new Slip BC, which also well capture the Re_τ variation.

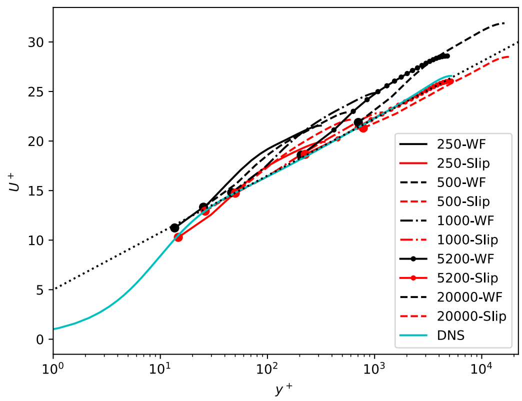

Figure 5. Mean velocity by the new Slip BC (red) compared with standard WF (black) and DNS for different Re_τ at different resolutions. The large dots represent the solutions in the first inner point.

The resolved Reynolds shear stress $\overline{u'v'}$ in Figure 6 shows, consistently with Figure 3, that there is a turbulent momentum flux present already at the boundary. For the lowest Reynolds numbers, though, the damping function in (12) is activated and the near-wall turbulence correspondingly damped. The damping appears to activate at relatively high Reynolds numbers though, suggesting that C_{s0}^+ could be reduced.

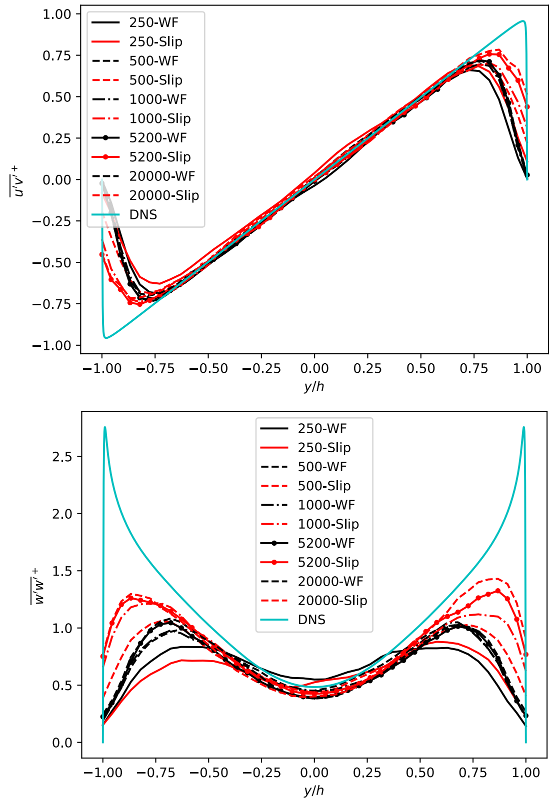

Figure 6. The resolved shear stress $\overline{u'v'}$ (top) and spanwise fluctuations $\overline{w'w'}$ (bottom) (as Figure 5).

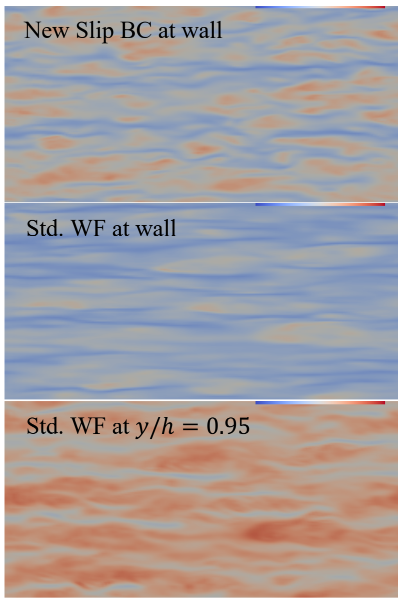

Figure 7. Instantaneous $u_x(x,z)$ at the wall boundary for the new Slip BC (top) and standard WF (middle and bottom) for the medium m mesh and Re_τ=5 200. The last figure is a cut at $0.05h$ from the wall.

CONCLUDING REMARKS

The new Slip BC for wall-modelled LES is principally different from the existing wall treatments for several reasons.

Firstly, the formulation is based on a simple Reynolds number scaling of the very near-wall conditions for a surrogate setup for an "LES fluid". It is also completely locally defined at the boundary without any explicit relation to the log law, nor any dependency of velocity in the interior of the flow.

Wall-functions for RANS, in contrast, are non-local with an explicit "hard-coded" log-law relation. In a RANS sense, they provide turbulence shear stress and production at the boundary. When these WFs are used for LES, they will only provide SGS (i.e. viscous) shear stress which need a transition (buffer) region to develop into resolved turbulence. RANS-based WFs are, in this respect, not suitable to be used for LES. Moreover, due to the non-locality and relation to the log law, elaborated non-equilibrium corrections are needed. We are expecting to see less need for such corrections for the proposed Slip BC. With the present approach we hope to see improvements in more complex flows far from equilibrium, e.g. pressure-induced flow separation.

Secondly, the Robin BC for the wall-normal fluctuation enables fluctuations at the boundary which correlates with the streamwise fluctuations resulting in resolved shear stress at the boundary with about the same order of magnitude as the SGS shear stress at the boundary. Hence, there is an explicit production of resolved turbulence energy already at the boundary, which is consistent with what is expected from the non-resolved high-Re buffer region. The turbulence-generating mechanism is passive, driven by the resolved turbulence in the vicinity of the boundary. Figure 7 shows instantaneous streamwise velocity at the BC. The typical "low-Re" streaks are seen for the standard WF with completely unphysical spacing (here $\Delta z^+ \approx 3000$). The new Slip BC shows a different pattern where the streaks are less pronounced. In fact, these wall structures are more similar as these seen at some distance from the wall for standard WF where the turbulence is more developed. This demonstrates that the proposed BC suppresses artificial near-wall streak spacing typical of under-resolved LES.

A similar slip BC, including wall-normal fluctuations, was proposed by Bose & Moin (2014) as a consequence of applying a differential LES filter (Germano 1986). Unlike such dynamic slip models, the present formulation derives the slip length from Reynolds-number similarity, resulting in reduced sensitivity to Reynolds number and grid resolution.

The new Slip BC was tested for a quite basic SGS model, the standard Smagorinsy model. More elaborated SGS models are superior in many aspects and the new BC can be applied for any SGS model as long as the SGS viscosity and the effective Smagorinsky constant C_S can be estimated close to the wall. However, some of these SGS models have some amount of near wall damping of the SGS viscosity, which is introducing some amount of effective wall slip. This wall slip is somewhat arbitrary and not connected to the Reynolds number scaling for the present Slip BC. Hence, there might be some interference between the Slip BC and the more advanced SGS model that must be considered and calibrated.

One final remark is based on the fact that the proposed wall BC is independent on the log law. Hence, the proposed Reynolds number scaling should be valid in the limit of DNS resolution as well. This means that it can provide the correct treatment of wall-resolved LES, or underresolved DNS, with arbitrary resolution just by the introduction of the proper wall slip boundary condition based on the Reynolds number scaling rather than the more common ad-hoc modifications.

One final remark is that the proposed wall boundary condition is not tied to the log law. The Reynolds-number scaling is formulated in terms of the computational viscosity and therefore naturally approaches the no-slip condition in the DNS limit $\nu^* \rightarrow \nu$. This suggests that the same framework can be consistently applied across resolutions, from wall-modelled LES to wall-resolved LES or mildly under-resolved DNS, without relying on ad-hoc modifications.

ACKNOWLEDGEMENT

This work was partly made within the National Aviation Research Programme, project LESisMORE "Large-Eddy Simulation In aeronautical applicationS; wall Modeling, rObustness, accuRacy and Efficiency" (NFFP, grant No. 2024-01295), with funding from Saab Aeronautics. Moreover, the work was partly made within the EU HORIZON-CL5 project ROSAS "RObust simulation Systems exploiting AI based turbulence models and high-fidelity algorithmS" funded by the European Union under Grant Agreement n°101138319. Finally, the computations were performed on resources provided by the National Academic Infrastructure for Supercomputing in Sweden (NAISS) at the Dardel supercomputer at PDC, KTH, Sweden.

REFERENCES

Muschinski, A., 1996, "A similarity theory of locally homogeneous and isotropic turbulence generated by a Smagorinsky-type LES", *J. Fluid Mech.* 325.

Reyes, D.A., Cooper, J.M. and Girimaji S.S., 2014, "Characterizing velocity fluctuations in partially resolved turbulence simulations", *Phys. Fluids* 26.

Bose, S.T. and Moin, P., 2014, "A dynamic slip boundary condition for wall-modeled large-eddy simulation", *Phys. Fluids* 26.

Germano, M., 1986, "Differential filters of elliptic type", *Phys. Fluids* 29.

Lācis U, Sudhakar Y, Pasche S, Bagheri S., 2020, Transfer of mass and momentum at rough and porous surfaces. *J. Fluid Mech*. 884. doi:10.1017/jfm.2019.897

Lozano-Durán A, Bae HJ., 2019, Characteristic scales of Townsend's wall-attached eddies. *J. Fluid Mech*. 868. doi:10.1017/jfm.2019.209

Habibi Khorasani SM, Lācis U, Pasche S, Rosti ME, Bagheri S., 2022, Near-wall turbulence alteration with the transpiration-resistance model. *J. Fluid Mech*. 942. doi:10.1017/jfm.2022.358